Optical and Quantum Electronics (2025) 57:626
https://doi.org/10.1007/s11082-025-08556-8

Symmetrically etched plastic optical fiber sensor for the detection of ethylene glycol contamination in water

Rana M. Armaghan Ayaz[1] · Adil Mustafa[2,3] · Riccardo Funari[1]

Received: 12 August 2025 / Accepted: 28 October 2025 / Published online: 10 November 2025
© The Author(s) 2025

Abstract
Human activities are increasingly contaminating surface and groundwater reserves. Among various pollutants, ethylene glycol (EG) contamination in water is particularly dangerous. At low concentrations it can enter the body undetected and causes serious health problems such as kidney failure and gastrointestinal disorders. This study demonstrates the use of symmetrically etched single-mode plastic optical fiber (POF) sensor model operating at 1550 nm for detecting EG presence in water using COMSOL Multiphysics. The working of the sensor is based on evanescent field interactions with surrounding medium to detect refractive index (RI) changes, while transmission variations through etched POF serving as the sensing metric. Simulations were conducted for aqueous EG solutions ranging from 0 to 0.15 weight fraction, corresponding to RI values ranging between 1.316 and 1.330. The sensor design was optimized by examining the impact of etched cladding diameter and etched length on sensitivity. These parameters were varied from 60 to 7.05 and 1 to 30 μm, respectively. This in turn lead to sensitivity values in the range of 0.39×10^{-3} to 99.50×10^{-3} Trans. (A.U)/RIU. Highlighting the importance of evanescent field-surrounding interaction for etched POF sensors, these findings revealed that sensitivity has direct relation with the length of etched region and inverse relation with cladding diameter. The maximum sensitivity of 99.50×10^{-3} Trans. (A.U)/RIU was achieved with a 30 μm etched length and 7.05 μm cladding diameter. The proposed POF-based sensor demonstrates strong potential for applications in biomedical engineering, biochemical monitoring, and beverage industry offering a compact and sensitive solution for EG contamination detection in water.

Keywords Plastic optical fiber · Water contamination · Evanescent field · Single mode · Symmetrical etching · Penetration depth

Extended author information available on the last page of the article

1 Introduction

In recent years, various contaminants have infiltrated all types of water bodies, including surface water, groundwater, drinking water, and even precipitation (Khan et al. 2022; Sharma and Bhattacharya 2017). Among the various pollutants, contamination by ethylene glycol (EG) is of particular concern. EG is a colorless, odorless, and viscous liquid with a sweet taste, posing significant health risks when ingested over prolonged periods (Staples et al. 2001; Abdelghani et al. 1990). Children are especially vulnerable to EG poisoning due to its appealing flavor, often leading to accidental ingestion. Common sources of EG pollution include antifreeze solutions, hydraulic brake fluids, and cooling systems in automotive applications. To address this issue, several analytical techniques have been employed for EG detection in water, including chromatography, near-infrared (NIR) spectroscopy, and Fourier-transform infrared (FTIR) spectroscopy (Tran et al. 2014; Holland et al. 2022; Khalique Ahmed et al. 2010). Although these methods are mature and highly reliable, but they typically require expensive and complex instrumentation, as well as skilled personnel for proper operation, thereby limiting their application for real-time water quality monitoring (Bao et al. 2015). Given the challenges associated with EG detection, particularly due to its physicochemical characteristics, there has been growing interest in the development of low-cost, portable, user-friendly, and compact sensors. This demand has paved the way for evanescent field-based optical fiber sensing techniques for monitoring EG pollution in aqueous environments. Optical fiber sensors offer several advantages over electronic transducers, including immunity to electromagnetic interference, compact size, and resilience in harsh environmental conditions (Giallorenzi et al. 1982; Lee 2003).

Evanescent field glass optical fiber (EF-GOF) sensors operate by detecting changes in the refractive index (RI) resulting from the interaction of the evanescent field, emanating from the fiber core, with the surrounding medium (Memon et al. 2017; Khijwania et al. 2005; Funari et al. 2025). Tapering and side polishing of SMF are some of the most common approaches that have been explored to enhance this interaction by reducing diameter of the fiber, thereby increasing the strength of the evanescent field in the sensing region (Leung et al. 2007; Zhao et al. 2020; Villatoro et al. 2003). However, these modifications introduce some major challenges such as lower numerical aperture, reduced durability in humid or chemically aggressive environments, increased fragility, and higher costs, constraining the broader application of EF-GOF sensors (Golnabi and Azimi 2007; Zubia and Arrue 2001; Butt et al. 2022). In this context, plastic optical fibers (POFs) have recently emerged as a promising alternative, effectively addressing many of the limitations associated with conventional EF-GOF sensors. POFs, in addition to offering the classical advantages of glass optical fibers (GOFs), are cost-effective, flexible, easy to handle and fabricate. They also possess a larger numerical aperture and do not require additional protective coatings against corrosive chemicals, oils, or industrial solvents (Wang and Wolfbeis 2016; Bilro et al. 2012; Chen et al. 2018). Though POFs typically experience higher transmission losses compared to GOFs, but this characteristic can be beneficial in fiber sensor design, particularly by enhancing evanescent field interactions.

While several optical sensors for EG detection in water have been reported in the literature (Panda and Pukhrambam 2021; Martínez et al. 2023), but to the best of the authors' knowledge, none of these studies have utilized evanescent field interaction principle occurring at 1550 nm wavelength in single-mode POFs. Most of the evanescent field plastic

optical fiber (EV-POF) sensors with enhanced evanescent field strength achieved through structural modifications, have primarily been applied in biosensing, gas detection, and temperature monitoring (Gravina et al. 2009; Bartlett et al. 2000). For instance, in Moraleda et al. (2013), researchers demonstrated a POF macrobend-based temperature sensor with a sensitivity of $1.92 \times 10^{-3}\,(^{\circ}\mathrm{C})^{-1}$. Oxygen detection using a tapered polymethylmethacrylate (PMMA)-based POF was reported in Pulido and Esteban (2013). Similarly, (Batumalay et al. 2014) employed a tapered POF with ZnO nanostructures to enhance sensitivity for uric acid and relative humidity detection. Considering the challenges associated with POF tapers, Chu and Lo (2007) proposed a side-polished POF for simultaneous temperature and oxygen sensing. A side-polished POF was also utilized for a cure monitoring system in Bilro et al. (2010). However, side polishing techniques suffer from some significant drawbacks, such as uneven surface profiles, increased polarization-dependent losses, surface roughness, thermal softening, micro-cracks, and defects (Koeppen et al. 1998; Jing et al. 2014; Shahinian 2018; Al-Qazwini et al. 2016). Chemical etching has thus emerged as a more favorable approach for reducing fiber diameter and enhancing light–matter interaction. For example, Zhao et al. (2017) employed a simple wet etching technique using an aqueous acetic acid solution with ultrasonic irradiation to fabricate a glucose sensor, achieving a sensitivity of 9.10 $(\mathrm{RIU})(\mathrm{g/L})^{-1}$. In Bhowmik et al. (2014), the intrinsic sensing properties of single-mode POFs (S-POFs) were enhanced by etching to various diameters and subsequently inscribing Bragg gratings to measure strain, temperature, and pressure. As highlighted in the literature, most of the commercially available POFs operate in the visible wavelength (600–700 nm) Bartlett et al. (2000); Zubia and Arrue (2001), benefiting from lower attenuation and the wide availability of light sources (Koike and Asai 2009; Kuriki et al. 2002). However, this makes them incompatible with standard telecommunication fiber systems that operate in the infrared range, which offers reduced scattering and greater penetration depth. Moreover, the presence of background visible light can introduce noise, lowers the reliability and accuracy for the sensitive measurements (Koike and Koike 2011; Elsherif et al. 2022). In this study, a two-dimensional (2*D*) model of a single-mode plastic optical fiber (S-POF) based on cyclo-olefin polymer (COP) was developed using the Wave Optics Module in COMSOL Multiphysics and analyzed for its performance for detecting EG contamination in water at an operating wavelength of 1550 nm. COP is particularly valuable as a building block for POFs due to its ease of fabrication, lower loss in the near-infrared (NIR) region, and the tunability of its refractive index through simple co-polymerization or by mixing polymers of different grades (Shao et al. 2023; Snyder and Young 1978).

By modeling and simulating the symmetric etching conditions of proposed S-POF, design optimization was carried out by investigating the effects of cladding thickness and the length of the uniformly etched region on its transmission and, ultimately, on the sensor's sensitivity. For aqueous solutions of EG with weight having fractions varying from 0 to 0.15, the sensitivity ranging from 0.39×10^{-3} to 99.50×10^{-3} Trans. (A.U)/RIU was obtained, as the etched region length increased from 1 to 30 μm and the cladding diameter was reduced from 60 to 7.05 μm. These results indicate a strong dependence of sensitivity on both etched length and cladding diameter. The maximum sensitivity of approximately 99.50×10^{-3} Trans. (A.U)/RIU was observed for the presented sensor model with the 30 μm etched region and 7.05 μm cladding diameter, as its design parameters. This study can serve as a foundation for future work aimed at optimizing and amplify the performance of POF sensors for various sensing applications.

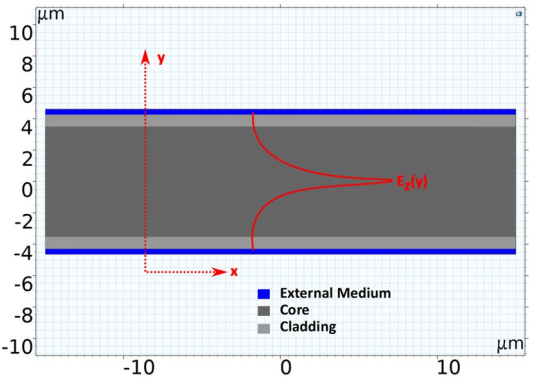

Fig. 1 Etched S-POF sensor model, designed and simulated in the 2*D* environment of COMSOL Multiphysics to investigate its ability for EG contamination detection in water. The core, cladding, and external medium regions are marked with distinct colors, and the direction of electric field propagation has been indicated by E_z

Table 1 Diameter and RI values used to model the single-mode evanescent field plastic optical fiber sensor (EV-POF) operating at the excitation wavelength of 1550 nm

Parameters	Diameter (µm)	Refractive index (RIU)
Core (n_{co})	7	1.535
Cladding (n_{cl})	60	1.525

2 Methodology

The two-dimensional (2*D*) POF model used in this study for detecting EG contamination in water via COMSOL Multiphysics has been depicted in Fig. 1. This model simulates a non-commercial POF design originally developed and used by Shao et al. (2023). In Fig. 1, the core and cladding are depicted in dark and light gray colors, respectively, while the sample under investigation is represented in blue. The proposed sensor model was simulated in the frequency domain using the Electromagnetic Waves, Frequency Domain (EWFD) interface in COMSOL Multiphysics. For this configuration, numeric port boundary conditions (N-PBCs), along with wave excitation port settings were applied to the left and right sides, designating the selected sides as Port 1 and Port 2. In our analysis, activating the excitation port setting for Port 1 made it as the input for the incoming wave, while Port 2 acts as the output when its excitation configuration is turned off. Scattering boundary conditions (SBCs) were applied to the top and bottom boundaries to allow waves to exit the simulation domain without reflection, ensuring accurate results. To achieve the numerical stability, computational efficiency and high accuracy, a physics-controlled mesh with a finer element size was used for meshing the model.

The detailed design parameters are given in Table 1.

Figure 2 shows the proposed experimental setup for detecting EG contamination in water.

For real-world implementation, the proposed sensing device as shown in Figs. 1 and 2 can be fabricated by symmetrically etching COP based POF by using specific solvents such as toluene, cyclohexane, or through techniques such as reactive ion etching, plasma etching or laser ablation (Snyder and Young 1978; Chiang 2003; Skelton et al. 2012). In practice, laser ablation combined with controlled exposure time and symmetric irradiation is generally preferred to minimize device-to-device variations (Snyder and Young 1978; Ahmad and Hench 2005). To enhance repeatability and performance, measures such as in-process diameter and transmission monitoring (via microscopy/laser micrometry), immediate DI-water

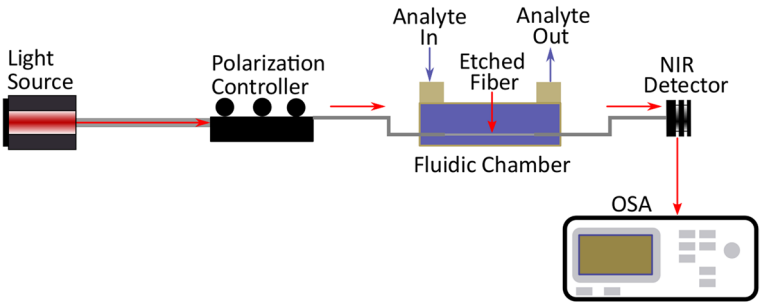

Fig. 2 Proposed setup for experimental study and performance evaluation of EG contamination sensor based on a symmetrically etched POF

quenching, post-etch surface/symmetry inspection, and encapsulation of the etched segment to stabilize alignment and reduce environmental drift are also recommended.

One way to describe the light propagation in a waveguide or an optical structure is through effective refractive index, denoted as n_{eff}. If c is the speed of light in a vacuum and v_{g} is its group velocity while propagating through a circular waveguide, then n_{eff} can be mathematically expressed as follows Snyder and Young (1978), Chiang (2003)

$$n_{\text{eff}} = \frac{c}{v_{\text{g}}} \tag{1}$$

When an excitation signal of wavelength λ propagates through the core of a S-POF with n_{eff} as effective index, a small fraction of its energy extends into the surrounding cladding region over a short distance, commonly known as the *penetration depth*, d_{p}. Eq. 2 given below, is usually used to calculate d_{p} Ahmad and Hench (2005), Skelton et al. (2012) as

$$d_{\text{p}} = \frac{\lambda}{2\pi\sqrt{n_{\text{eff}}^2 - n_{\text{cl}}^2}} \tag{2}$$

The refractive index $n_{\text{eq.}}$ for different weight fractions (w) of homogeneous ethylene aqueous solutions at an operational wavelength of 1550 nm can be estimated using the following empirical relation (Saunders et al. 2016)

$$n_{\text{real,EG}} = Aw^3 + Bw^2 + Cw + D \tag{3}$$

where the coefficients are: $A = -0.0223$, $B = 0.0321$, $C = 0.0910$, and $D = 1.3166$.

An increase in $n_{\text{eq.}}$ in the vicinity of the symmetrically etched region of the POF sensor (depicted as the blue area in the model) leads to a decrease in transmission intensity at the output. The change in transmission (ΔT) as a function of $n_{\text{eq.}}$ defines the *sensitivity* S of the proposed sensor, expressed in Trans. (A.U)/RIU, and is given by Eq. 4 De-Jun et al. (2014a, b)

$$S = \frac{\Delta T}{\Delta n_{\text{eq.}}} \tag{4}$$

In spatial refractive index distribution $n(x, y)$, the properties of guided mode having free-space wavenumber $k = \pi/\lambda$, propagation constant β and and effective index $n_{eff.} = \beta/k_o$ are obtained by solving the following Helmholtz equation for the electric field distribution $E(x, y)$ (Feit and Fleck 1980a, b)

$$\nabla^2 E = k_o^2 n^2(x, y)E = \beta^2 E \tag{5}$$

3 Results and discussions

Our analysis began by examining the profile of the guided mode through a 30 µm long POF, both in its non-etched form and when symmetrically etched on both sides with air as the surrounding medium. The results of this step are illustrated in Fig. 3. As shown in Fig. 3a–c, when the POF is non-etched, the evanescent field of the guided mode remains strongly confined within the cladding region and decays there without interacting with the external environment. The computed full width at half maximum (FWHM) of fundamental guided mode LP_{01} of around 9.14 µm, in non-etched fiber obtained by applying Lorentzian fitting with 1.5305 as its effective index $n_{eff.}$, also supports the stated fact. On the other hand, when the cladding is symmetrically etched from both sides and its diameter is reduced from 60 to 7.05 µm approximately 8.5 times smaller than the original, guided mode LP_{01} becomes less confined and a significant portion of the evanescent field from the guided mode extends into the surrounding sensing region, as illustrated in Fig. 33d–f. In contrast to strong confinement case, for the new condition, FWHM of weakly guided mode found by applying Lorentzian fitting came out to be approximately 12.26 µm with $n_{eff.}$ equal to 1.5265 . The presence of strong evanescent field in the vicinity is crucial for the effective operation of evanescent field-based fiber optic sensing mechanisms. Later, the performance of our pro-

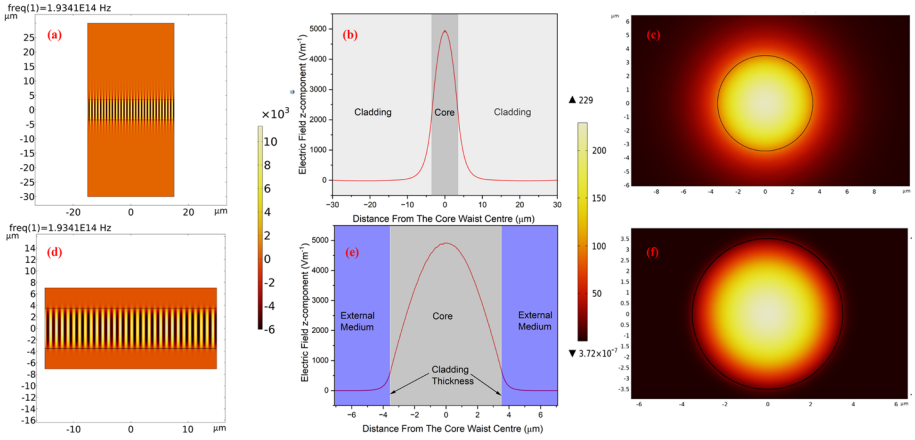

Fig. 3 For the 30 µm POF sensor model: **a** electric field *z*-component (V/m) and **b** guided mode profile for the non-etched fiber; **d** electric field *z*-component (V/m) and **e** guided mode profile for the fiber with cladding diameter reduced from 60 to 7.05 µm by symmetrical etching. Normalized electric field distribution in the cross-sectional view of the plastic optical fiber: **c** non-etched and **f** symmetrically etched to a cladding diameter of 7.05 µm, both in air

posed single-mode POF sensor was evaluated in detecting EG contamination in water. To establish a baseline, we began by considering the deionized (DI) water as the background medium in the sensing region, shown in blue color in Fig. 1. The refractive index of DI water was considered 1.316, which is a typical value reported for it at central wavelength of 1550 nm (Zhou et al. 2020; Saunders et al. 2016) . The real part of the refractive index of this background medium was gradually increased from 1.3166 to 1.330 in equal steps of 0.50×10^{-3} RIU by using Eq. 3. Throughout this process, the transmission was recorded as a function of the refractive index change, and the sensitivity was calculated with the help of Eq. 4. This RI range was selected as it corresponds to an EG weight fraction of 0–0.15 in aqueous solution. This concentration range is particularly relevant because EG can enter the body unnoticed and cause serious health issues such as kidney damage and gastrointestinal disorders (Hess et al. 2004; Caravati et al. 2005).

At this stage, the effect of fiber length and cladding diameter on the sensor's sensitivity was also thoroughly examined as part of a design optimization effort. The objective was achieved by implementing parametric sweep function provided in COMSOL Multiphysics for varying the length of the symmetrically etched region of the POF sensor from 1 to 30 µm with the regular interval size of 5 µm and evaluating the sensitivity for each model while reducing the cladding diameter with the help of another parametric sweep defined for it. The latter sweep function was set to reduce the cladding diameter from its original value of 60 µm to as low as 7.05 µm (8.5 times smaller) having cladding diameter reduction factor of 0.5 as its step size. The results of this investigation are summarized in Fig. 4.

An almost linear drop in transmission was measured with increasing EG concentration in water. The slopes of the typical transmission patterns shown in Fig. 4a–c, obtained for a

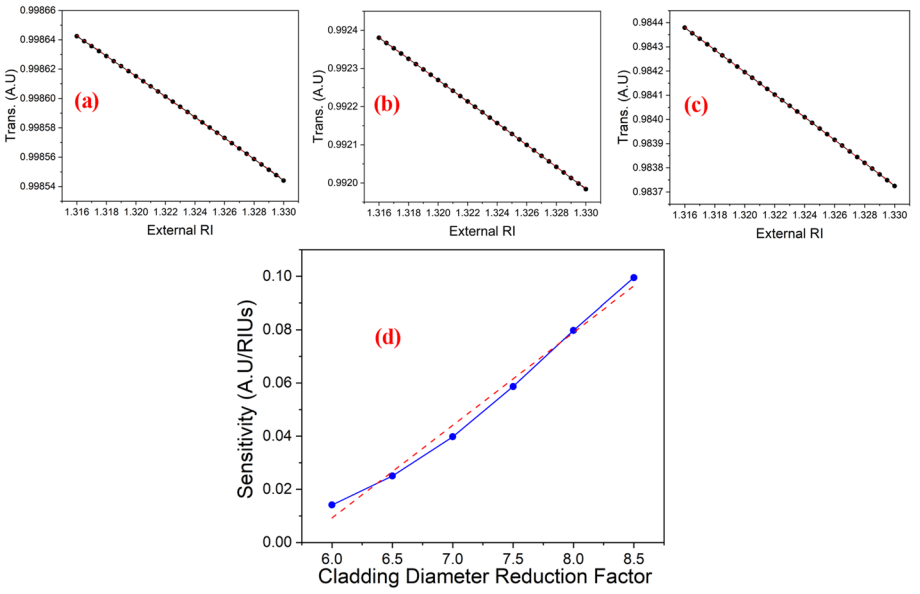

Fig. 4 Reduction in transmission (black color line) with applied fitting (red color line) for a 15 µm long, uniformly and symmetrically etched POF sensor model at **a** 10 µm, **b** 8 µm, and **c** 7.50 µm cladding diameters, respectively. **d** Increase in sensitivity (blue line) with applied linear fit (red line) for a 30 µm long uniformly and symmetrically etched POF sensor, as the ratio of original to etched cladding diameter also knows as cladding diameter reduction factor, was increased from 6.0 to 8.5

15 µm long symmetrically etched POF while its cladding diameter was decreased from 10 to 7.50 µm, demonstrate that for a fixed etched length, sensitivity increases gradually from 7.02×10^{-3} Trans. (A.U)/RIU to 38.77×10^{-3} Trans. (A.U)/RIU with the reduction of the POF cladding diameter. This is due to the fact that reducing the cladding diameter allows more of the guided optical mode to extend outside the fiber core, thereby increasing the evanescent field strength and its overlap with the surrounding medium. Similarly, Fig. 4d was obtained from the detailed analysis of a 30 µm symmetrically etched POF, further shows that in addition to the reduced cladding diameter, the increased length of the etched region also contributes to improved sensitivity. This occurs because a longer etched region exposes more of the optical field to the external medium, increasing the extent of light–environment interaction and leading to higher attenuation or loss over longer interaction lengths. To validate these observations, a more rigorous analysis was conducted by considering various lengths and diameters of the etched region, which led to the results presented in Fig. 5.

Starting from 0.39×10^{-3} Trans. (A.U)/RIU, obtained for 1 µm etched length at 10 µm etched diameter, an almost linear increase in sensitivity as a function of increase in etched length and cladding diameter reduction factor was recorded. From this behavior, it can be inferred that, for the proposed EG water contamination sensor model, sensitivity has a direct relationship with the symmetrically etched region and an inverse relationship with the cladding diameter. These findings not only support the aforementioned observations but also align well with the results reported by Ji et al. (2020) and Razali et al. (2022), who investigated the effect of cladding thickness on sensor performance. Table 2 summarizes the outcomes derived from the design optimization stage conducted for the presented symmetrically etched POF-based EG water contamination sensor. Under the optimal design conditions, comprising of 7.05 µm etched cladding diameter and 30 µm etched length, the proposed optical sensor achieved a maximum sensitivity of approximately 99.50×10^{-3} Trans. (A.U)/RIU.

Table 3 provides a comparison of presented work with previously available studies.

The proposed POF sensor model for EG contamination detection in water demonstrates strong potential for real-world applications across multiple sectors. Its high sensitivity, compact size, and evanescent field-based detection mechanism make it particularly suitable for on-site and real-time monitoring. Such a sensing platform can find its widespread deployment in the fields of biomedical engineering, biochemistry, environmental monitoring and public health surveillance.

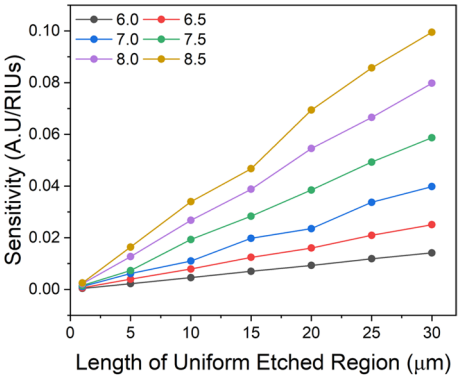

Fig. 5 Effect of symmetrically etched POF length and its diameter on the sensitivity of the proposed water contamination detection sensor model. The figure legend indicates the ratio between the original cladding diameter and the reduced etched diameter

Table 2 Sensitivity (Trans. (A.U)/RIU) of the symmetrically etched POF sensor for ethylene glycol contamination detection in water, evaluated at various etched cladding diameters and lengths

Cladding diameter reduction factor (original/etched)	Sensitivity (1×10^{-3}Trans. (A.U)/RIU) of symmetrically etched fiber lengths (μm)						
	1 μm	5 μm	10 μm	15 μm	20 μm	25 μm	30 μm
6.0	0.39	2.23	4.57	7.02	9.27	11.86	14.13
6.5	0.63	3.97	7.89	12.42	16.02	20.95	25.04
7.0	1.10	6.14	11.00	19.77	23.50	33.70	39.78
7.5	1.51	7.30	19.29	28.32	38.45	49.26	58.68
8.0	2.18	12.67	26.73	38.77	54.53	66.52	79.79
8.5	2.51	16.37	33.94	46.72	69.38	85.69	99.50

Table 3 Comparison of different POF-based sensing structures reported in literature with the present work

POF Structure	Sensitivity	Operating λ (nm)	RI Range	References
Double-sided polished	4284.8 nm/RIU	600–900	1.34–1.42	Liu et al. (2021)
Single-side polished	219.504 dBm/RIU	1540–1600	1.33–1.35	Zhang et al. (2021)
Mach–Zehnder interferometer	84 MHz/RH	1530–1570	–	Cheng et al. (2021)
Polymer-based	0.0083 dB/RH	500–650	–	Lu et al. (2021)
Fiber Bragg grating	1.27 ± 0.01 pm/με	1526–1576	–	Pospori et al. (2022)
Flat-POF	2507 nm/RIU	400–1000	1.33–1.39	Xue et al. (2022)
Our work	99.50×10^{-3} /RIU	1550	1.31–1.33	–

4 Conclusion

The design and simulation of COP-based, single-mode, symmetrically etched POF sensor operating at a wavelength of 1550 nm for detecting EG contamination in water, within the weight fraction range of 0–0.15, have been demonstrated. For real-world implementation, such COP-based POF sensors can be fabricated using reactive ion etching or laser ablation techniques. The optimization process was carried out through parametric sweeps of the etched length and diameter, showing that the sensitivity of the POF sensor is directly proportional to the etched length and inversely proportional to the etched diameter. Optimal performance was achieved with an etched diameter of 7.05 μm and an etched length of 30 μm, yielding a maximum sensitivity of approximately 99.50×10^{-3} Trans. (A.U)/RIU. The proposed symmetrically etched, COP-based POF sensor, validated through COMSOL Multiphysics simulations, demonstrates strong potential for applications in the food and biochemical industries, where high sensitivity and cost-effective detection tools are essential.

Author Contributions Rana M. Armaghan did conception of idea, design, simulations, data collection, analysis, comparison and wrote the whole manuscript. Adil Mustafa contributed to data analysis from initial simulations, read and suggested improvements in the final manuscript. Riccardo Funari contributed to data analysis from initial simulations, read and suggested improvements in the initial version and final manuscript. All authors reviewed and approved the final manuscript.

Funding Open access funding provided by Scuola Superiore Sant'Anna within the CRUI-CARE Agreement. The authors declare that no funds, grants, or other support were received during the study or for the preparation of this manuscript.

Data Availability Data will be made available upon request.

Declarations

Conflict of interest The authors have no relevant financial or non-financial interests to disclose.

Open Access This article is licensed under a Creative Commons Attribution 4.0 International License, which permits use, sharing, adaptation, distribution and reproduction in any medium or format, as long as you give appropriate credit to the original author(s) and the source, provide a link to the Creative Commons licence, and indicate if changes were made. The images or other third party material in this article are included in the article's Creative Commons licence, unless indicated otherwise in a credit line to the material. If material is not included in the article's Creative Commons licence and your intended use is not permitted by statutory regulation or exceeds the permitted use, you will need to obtain permission directly from the copyright holder. To view a copy of this licence, visit http://creativecommons.org/licenses/by/4.0/.

References

Abdelghani, A., Anderson, A., Khoury, G., Chang, S., et al.: Fate of ethylene glycol in the environment. Technical report. Tulane University, School of Public Health and Tropical Medicine (1990)

Ahmad, M., Hench, L.L.: Effect of taper geometries and launch angle on evanescent wave penetration depth in optical fibers. Biosens. Bioelectron. **20**(7), 1312–1319 (2005)

Al-Qazwini, Y., Noor, A., Al-Qazwini, Z., Yaacob, M.H., Harun, S.W., Mahdi, M.: Refractive index sensor based on spr in symmetrically etched plastic optical fibers. Sens. Actuators, A **246**, 163–169 (2016)

Bao, L.-J., Wei, Y.-L., Yao, Y., Ruan, Q.-Q., Zeng, E.Y.: Global trends of research on emerging contaminants in the environment and humans: a literature assimilation. Environ. Sci. Pollut. Res. **22**, 1635–1643 (2015)

Bartlett, R.J., Philip-Chandy, R., Eldridge, P., Merchant, D.F., Morgan, R., Scully, P.J.: Plastic optical fibre sensors and devices. Trans. Inst. Meas. Control. **22**(5), 431–457 (2000)

Batumalay, M., Harith, Z., Rafaie, H., Ahmad, F., Khasanah, M., Harun, S., Nor, R., Ahmad, H.: Tapered plastic optical fiber coated with zno nanostructures for the measurement of uric acid concentrations and changes in relative humidity. Sens. Actuators, A **210**, 190–196 (2014)

Bhowmik, K., Peng, G.-D., Ambikairajah, E., Lovric, V., Walsh, W.R., Prusty, B.G., Rajan, G.: Intrinsic high-sensitivity sensors based on etched single-mode polymer optical fibers. IEEE Photonics Technol. Lett. **27**(6), 604–607 (2014)

Bilro, L., Alberto, N., Pinto, J., Nogueira, R.: A simple and low-cost cure monitoring system based on a side-polished plastic optical fibre. Meas. Sci. Technol. **21**(11), 117001 (2010)

Bilro, L., Alberto, N., Pinto, J.L., Nogueira, R.: Optical sensors based on plastic fibers. Sensors **12**(9), 12184–12207 (2012)

Butt, M.A., Voronkov, G.S., Grakhova, E.P., Kutluyarov, R.V., Kazanskiy, N.L., Khonina, S.N.: Environmental monitoring: a comprehensive review on optical waveguide and fiber-based sensors. Biosensors **12**(11), 1038 (2022)

Caravati, E.M., Erdman, A.R., Christianson, G., Manoguerra, A.S., Booze, L.L., Woolf, A.D., Olson, K.R., Chyka, P.A., Scharman, E.J., Wax, P.M., et al.: Ethylene glycol exposure: an evidence-based consensus guideline for out-of-hospital management. Clin. Toxicol. **43**(5), 327–345 (2005)

Chen, H., Buric, M., Ohodnicki, P.R., Nakano, J., Liu, B., Chorpening, B.T.: Review and perspective: Sapphire optical fiber cladding development for harsh environment sensing. Appl. Phys. Rev. **5**(1), 011102 (2018)

Cheng, X., Hu, J., Zhu, K. and Zhao, Z.: High-resolution polymer optical fibre humidity sensor utilizing single-passband microwave photonic filter. Measurement **179**, 109462 (2021)

Chiang, K.: Construction of refractive-index profiles of planar dielectric waveguides from the distribution of effective indexes. J. Lightwave Technol. **3**(2), 385–391 (2003)

Chu, C.-S., Lo, Y.-L.: A plastic optical fiber sensor for the dual sensing of temperature and oxygen. IEEE Photonics Technol. Lett. **20**(1), 63–65 (2007)

De-Jun, F., Mao-Sen, Z., Liu, G., Xi-Lu, L., Dong-Fang, J.: D-shaped plastic optical fiber sensor for testing refractive index. IEEE Sens. J. **14**(5), 1673–1676 (2014a)

De-Jun, F., Guan-Xiu, L., Xi-Lu, L., Ming-Shun, J., Qing-Mei, S.: Refractive index sensor based on plastic optical fiber with tapered structure. Appl. Opt. **53**(10), 2007–2011 (2014b)

Elsherif, M., Salih, A.E., Muñoz, M.G., Alam, F., AlQattan, B., Antonysamy, D.S., Zaki, M.F., Yetisen, A.K., Park, S., Wilkinson, T.D., et al.: Optical fiber sensors: working principle, applications, and limitations. Adv. Photon. Res. **3**(11), 2100371 (2022)
Feit, M., Fleck, J., Jr.: Mode properties and dispersion for two optical fiber-index profiles by the propagating beam method. Appl. Opt. **19**(18), 3140–3150 (1980)
Feit, M., Fleck, J., Jr.: Computation of mode properties in optical fiber waveguides by a propagating beam method. Appl. Opt. **19**(7), 1154–1164 (1980)
Funari, R., Ayaz, R.M.A., Di Pasquale, F., Oton, C.J.: Design and fabrication of short-period long period gratings for refractive index sensing. Opt. Express **33**(14), 29786–29801 (2025)
Giallorenzi, T.G., Bucaro, J.A., Dandridge, A., Sigel, G.H., Cole, J.H., Rashleigh, S.C., Priest, R.G.: Optical fiber sensor technology. IEEE Trans. Microw. Theory Tech. **30**(4), 472–511 (1982)
Golnabi, H., Azimi, P.: Design and performance of a plastic optical fiber leakage sensor. Opt. Laser Technol. **39**(7), 1346–1350 (2007)
Gravina, R., Testa, G., Bernini, R.: Perfluorinated plastic optical fiber tapers for evanescent wave sensing. Sensors **9**(12), 10423–10433 (2009)
Hess, R., Bartels, M.J., Pottenger, L.H.: Ethylene glycol: an estimate of tolerable levels of exposure based on a review of animal and human data. Arch. Toxicol. **78**(12), 671–680 (2004)
Holland, T., Karunanithy, R., Mandrell, C., Abdul-Munaim, A.M., Watson, D.G., Sivakumar, P.: Observation of a signal suppressing effect in a binary mixture of glycol-water contamination in engine oil with fourier-transform infrared spectroscopy. Standards **2**(4), 474–483 (2022)
Ji, L., Yang, S., Shi, R., Fu, Y., Su, J., Wu, C.: Polymer waveguide coupled surface plasmon refractive index sensor: a theoretical study. Photon. Sens. **10**, 353–363 (2020)
Jing, N., Zheng, J., Zhao, X., Teng, C.: Refractive index sensing based on a side-polished macrobending plastic optical fiber. IEEE Sens. J. **15**(5), 2898–2901 (2014)
Khalique Ahmed, M., McLeod, M.P., Nézivar, J., Giuliani, A.W.: Fourier transform infrared and near-infrared spectroscopic methods for the detection of toxic diethylene glycol (DEG) contaminant in glycerin based cough syrup. Spectroscopy **24**(6), 601–608 (2010)
Khan, S., Naushad, M., Govarthanan, M., Iqbal, J., Alfadul, S.M.: Emerging contaminants of high concern for the environment: current trends and future research. Environ. Res. **207**, 112609 (2022)
Khijwania, S.K., Srinivasan, K.L., Singh, J.P.: An evanescent-wave optical fiber relative humidity sensor with enhanced sensitivity. Sens. Actuators B Chem. **104**(2), 217–222 (2005)
Koeppen, C., Shi, R., Chen, W., Garito, A.: Properties of plastic optical fibers. JOSA B **15**(2), 727–739 (1998)
Koike, Y., Asai, M.: The future of plastic optical fiber. NPG Asia Mater. **1**(1), 22–28 (2009)
Koike, Y., Koike, K.: Progress in low-loss and high-bandwidth plastic optical fibers. J. Polym. Sci., Part B: Polym. Phys. **49**(1), 2–17 (2011)
Kuriki, K., Koike, Y., Okamoto, Y.: Plastic optical fiber lasers and amplifiers containing lanthanide complexes. Chem. Rev. **102**(6), 2347–2356 (2002)
Lee, B.: Review of the present status of optical fiber sensors. Opt. Fiber Technol. **9**(2), 57–79 (2003)
Leung, A., Shankar, P.M., Mutharasan, R.: A review of fiber-optic biosensors. Sens. Actuators B Chem. **125**(2), 688–703 (2007)
Liu, L., Deng, S., Zheng, J., Yuan, L., Deng, H. and Teng, C.: An enhanced plastic optical fiber-based surface plasmon resonance sensor with a double-sided polished structure. Sens. **21**(4), 1516 (2021)
Lu, X., Hicke, K., Breithaupt, M., & Strangfeld, C.: Distributed humidity sensing in concrete based on polymer optical fiber. Polym. **13**(21), 3755 (2021)
Martínez, E.E.G., Hualde-Otamendi, M., Zamarreño, C.R., Matías, I.R.: LMR-based optical sensor for ethylene detection at visible and mid-infrared regions. IEEE Sens. Lett. **7**(8), 1–4 (2023)
Memon, S.F., Ali, M.M., Pembroke, J.T., Chowdhry, B.S., Lewis, E.: Measurement of ultralow level bioethanol concentration for production using evanescent wave based optical fiber sensor. IEEE Trans. Instrum. Meas. **67**(4), 780–788 (2017)
Moraleda, A.T., García, C.V., Zaballa, J.Z., Arrue, J.: A temperature sensor based on a polymer optical fiber macro-bend. Sensors **13**(10), 13076–13089 (2013)
Panda, A., Pukhrambam, P.D.: Design and analysis of porous core photonic crystal fiber based ethylene glycol sensor operated at infrared wavelengths. J. Comput. Electron. **20**(2), 943–957 (2021)
Pospori, A., Ioannou, A. and Kalli, K.: Temperature and humidity sensitivity of polymer optical fibre sensors tuned by pre-strain. Sens. **22**(19), 7233 (2022)
Pulido, C., Esteban, Ó.: Tapered polymer optical fiber oxygen sensor based on fluorescence-quenching of an embedded fluorophore. Sens. Actuators B Chem. **184**, 64–69 (2013)
Razali, N.M., Ambran, S., Holmes, C., Zuikafly, S.N.F., Lokman, M.Q., Yuzir, A., Sapingi, H.H.J.: Design optimisation of c-shaped optical fibre sensor. Opt. Quant. Electron. **54**(7), 421 (2022)
Saunders, J.E., Sanders, C., Chen, H., Loock, H.-P.: Refractive indices of common solvents and solutions at 1550 nm. Appl. Opt. **55**(4), 947–953 (2016)

Shahinian, H.: Fiber based tools for polishing optical materials. PhD thesis, The University of North Carolina at Charlotte (2018)
Shao, Q., Dong, B., Li, K., Zhang, Z., Li, X., Yang, L., Chen, Z., Zhang, S.: Flexible single-mode polymer optical fiber-based modal interferometer for high-sensitivity bending measurement. IEEE J. Sel. Top. Quant. Electron. **30**(3: Flexible Optoelectronics), 1–7 (2023)
Sharma, S., Bhattacharya, A.: Drinking water contamination and treatment techniques. Appl Water Sci **7**(3), 1043–1067 (2017)
Skelton, S., Sergides, M., Patel, R., Karczewska, E., Maragó, O., Jones, P.: Evanescent wave optical trapping and transport of micro-and nanoparticles on tapered optical fibers. J. Quant. Spectrosc. Radiat. Transf. **113**(18), 2512–2520 (2012)
Snyder, A.W., Young, W.R.: Modes of optical waveguides. J. Opt. Soc. Am. **68**(3), 297–309 (1978)
Staples, C.A., Williams, J.B., Craig, G.R., Roberts, K.M.: Fate, effects and potential environmental risks of ethylene glycol: a review. Chemosphere **43**(3), 377–383 (2001)
Tran, B.N., Okoniewski, R., Bucciferro, A., Jansing, R., Aldous, K.M.: Determination of trace amounts of ethylene glycol and its analogs in water matrixes by liquid chromatography/tandem mass spectrometry. J. AOAC Int. **97**(1), 232–237 (2014)
Villatoro, J., Monzón-Hernández, D., Mejía, E.: Fabrication and modeling of uniform-waist single-mode tapered optical fiber sensors. Appl. Opt. **42**(13), 2278–2283 (2003)
Wang, X.-D., Wolfbeis, O.S.: Fiber-optic chemical sensors and biosensors (2013–2015). Anal. Chem. **88**(1), 203–227 (2016)
Xue, P., Xu, Y., Qi, J., Liu, Z. and Zhang, R.: Mechanically hot-pressed flattened plastic optical fiber-based SPR sensor and its RI sensing. Opt. Commun. **522**, 128635 (2022)
Zhang, X., Yang, B., Jiang, J., Liu, K., Fan, X., Liu, Z., Peng, M., Chen, G. and Liu, T.: Side-polished SMS based RI sensor employing macro-bending perfluorinated POF. Opto-Electron. Advant. **4**(10), 200041–1 (2021)
Zhao, M., Dai, L., Zhong, N., Wang, Z., Chen, M., Li, B., Luo, B., Tang, B., Shi, S., Song, T., et al.: Wet etching technique for fabrication of a high-quality plastic optical fiber sensor. Appl. Opt. **56**(31), 8845–8850 (2017)
Zhao, Y., Zhao, J., Zhao, Q.: Review of no-core optical fiber sensor and applications. Sens. Actuators A **313**, 112160 (2020)
Zhou, F., Su, H., Joe, H.-E., Jun, M.B.-G.: Temperature insensitive fiber optical refractive index probe with large dynamic range at 1,550 nm. Sens. Actuators A **312**, 112102 (2020)
Zubia, J., Arrue, J.: Plastic optical fibers: an introduction to their technological processes and applications. Opt. Fiber Technol. **7**(2), 101–140 (2001)

Publisher's Note Springer Nature remains neutral with regard to jurisdictional claims in published maps and institutional affiliations.

Authors and Affiliations

Rana M. Armaghan Ayaz[1] · Adil Mustafa[2,3] · Riccardo Funari[1]

✉ Rana M. Armaghan Ayaz
r.ayaz@santannapisa.it

Adil Mustafa
a.mustafa@bolton.ac.uk

Riccardo Funari
riccardo.funari@santannapisa.it

[1] Institute of Mechanical Intelligence, Scuola Superiore Sant'Anna, Via G. Moruzzi 1, 56124 Pisa, Italy

[2] School of Biomedical Sciences, University of Bristol, University Walk, Tankards Cl, BS8 1TL, Bristol BS8 1TL, UK

[3] School of Biomedical Engineering, University of Bolton, Deans Road, Bolton BL3 5AB, UK